# Supporting Information

## Fully Integrated Indium Gallium Zinc Oxide $NO_2$ Gas Detector

Mani Teja Vijjapu[1‡], Sandeep G. Surya[1‡], Saravanan Yuvaraja[1], Xixiang Zhang[2], Husam N. Alshareef[2], and Khaled N. Salama[*1]

[1]Sensors lab, Advanced Membranes and Porous Materials Center, Computer, Electrical and Mathematical Science and Engineering Division, King Abdullah University of Science and Technology (KAUST), Thuwal, 23955-6900, Kingdom of Saudi Arabia

[2]Physical Sciences and Engineering Division, King Abdullah University of Science and Technology (KAUST), Thuwal, 23955-6900, Kingdom of Saudi Arabia

## SI-1. Fabrication flow of the IGZO TFT

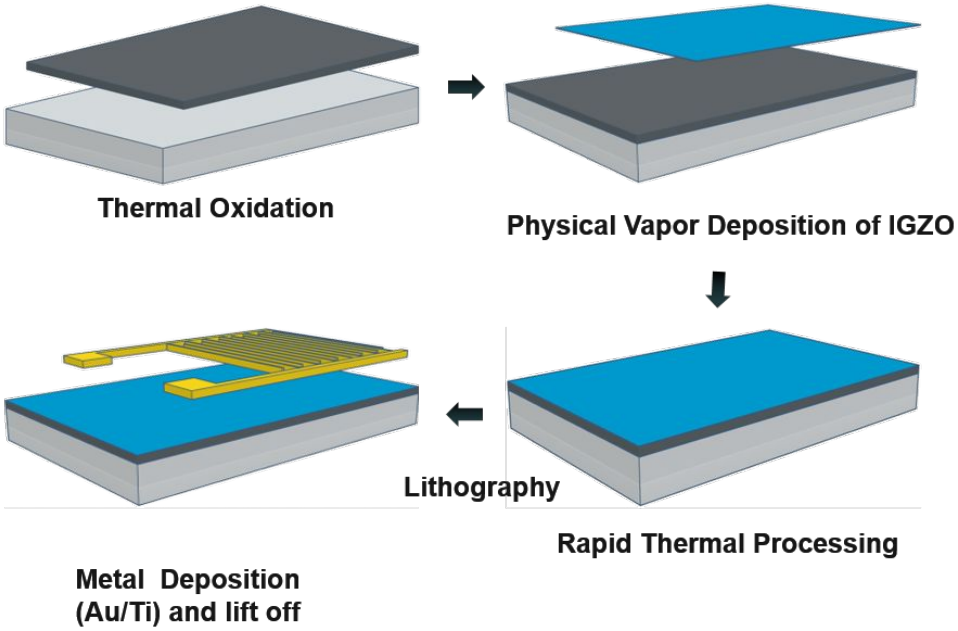


Figure S1. Fabrication flow of IGZO TFT

We purchased n-type doped Silicon wafers with (100) orientation from Silicon Materials (Si-MAT), served as the bottom Gate electrode. Si wafers were thoroughly cleaned to remove the organic and metal impurities by dipping them in the Piranha solution for five minutes. Followed by native oxide etch using buffered oxide etch solution. Subsequently, Silicon Oxide ($SiO_2$) 150 nm was deposited through the thermal oxidation in the thermal furnace at the KAUST Nanofab served as Gate oxide for the IGZO TFT. IGZO thin film (~10 nm) was deposited by RF sputtering using IGZO target ($In_2O_3$-$Ga_2O_3$-ZnO 1:1:2 mol%) supplied by Testbourne Ltd., UK. The sputtering was performed at 60W RF Power in the presence of Argon/Oxygen (20 SCCM/3 SCCM) plasma at 5 mtorr deposition pressure. Rapid Thermal Processing (RTP), to improve the TFT device stability, RTP has been done at $500^0$C for 4 minutes in the Oxygen ambience. Interdigitated top electrodes Titanium (Ti) / Gold (Au) was deposited using the lift-off process followed by the photolithography process to pattern interdigitated electrodes. The metal deposition has been done through the DC magnetron sputtering at 400W in the presence of Ar plasma to yield 10 nm and 100nm thickness of Ti and Au, respectively.

## SI-2. Thin-film transistor device Parameter extraction and calculations

Devices parameters were derived from the current equation as described in[1]. Linear Current equation ($I_{Dlin}$) and saturation Current ($I_{Dsat}$) for thin film transistor can be expressed as (Equation SE1 and SE2) :

$$I_{DLin} = \frac{\mu_{lin} * W * C_{ox}}{L} *((V_{GS}-V_{th}) * V_{DS} - (V_{DS}^2/2)) \quad \text{(SE1)}$$

$$I_{DSat} = \frac{\mu_{sat} * W * C_{ox}}{2 * L} *(V_{GS}-V_{th})^2 \quad \text{(SE2)}$$

where $C_{ox}$= Gate oxide capacitance; W=Width of the channel; L= length of the channel; $\mu_{lin}$ is the field-effect linear mobility; $\mu_{sat}$ is the field-effect saturation mobility.

*The subthreshold swing (SS)* was calculated from the linear $I_{DS}$- $V_{GS}$ curve using the formula (Equation SE3).

$$SS=\frac{dV_{GS}}{\mathrm{Log}_{10} * I_D|_{max}} \text{ (V/dec)} \quad \text{(SE3)}$$

It can be seen that current was decreasing with the increase in the concentration; hence, the subthreshold swing was increasing with the concentration of the exposed gas.

*Transconductance ($g_m$)* Transconductance is related to the conductance of the channel due to the accumulation of charges, and it was calculated from the linear regime of the device (Equation SE4).

$$g_m = \frac{dI_D}{dV_{GS}}|_{VDS < V_{GS}-V_{th}} (\Omega^{-1}) \quad \text{(SE4)}$$

With the increase in the concentration of $NO_2$, the transconductance was reducing due to the depletion of charge carriers.

*Linear Mobility* can be calculated using the $g_m$ Value. Since,

$$g_m = \frac{dI_D}{dV_{GS}}|_{VDS < V_{GS}-V_{th}} (\Omega^{-1}) = \frac{\mu_{lin} * W * C_{ox}}{L} * V_{DS};$$

$$\Rightarrow \mu_{Lin} = \frac{g_m * L}{W * V_{DS} * C_{ox}} \quad \text{(SE5)}$$

Mobility determines the transportation of charge carriers within the channel in the presence of an electric field. Scattering of the charge carriers near the dielectric interface or within channel affects its mobility. With the increase in the $NO_2$ concentration, mobility is reducing due to the decrease in transconductance, might also due to the scattering of charge carriers after exposure to $NO_2$ gas.

## SI-3. Test Setup

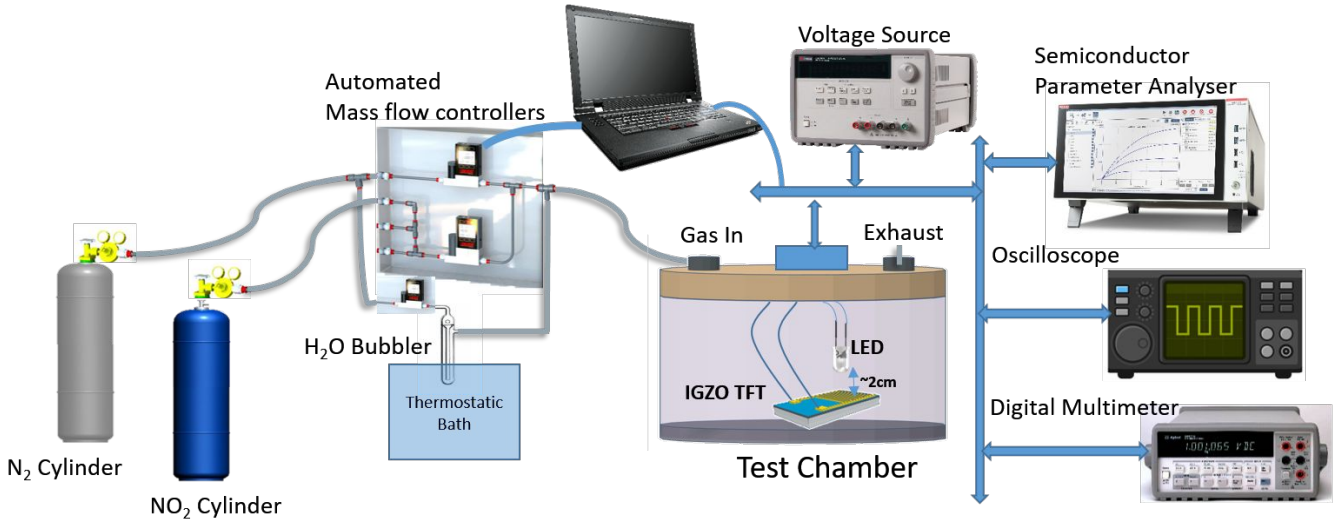


Figure S2. Schematic representation of test setup measuring IGZO TFT sensor with LED mounted at 2 cm above the active area.

## SI-4. Effect of $N_2$ presence during the revival

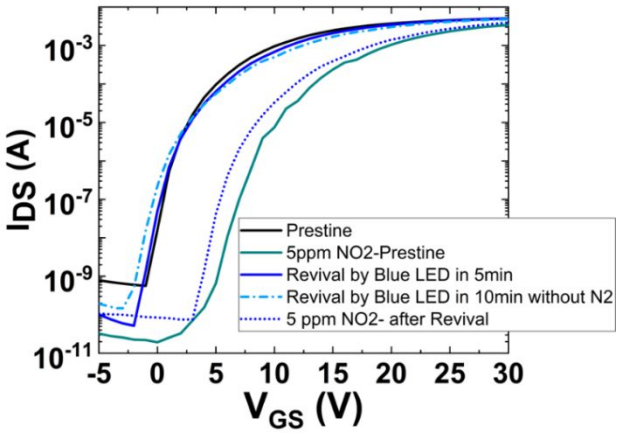


Figure S3. Transfer characteristics measured after exposure of 5 ppm $NO_2$, the revival of device in the presence of $N_2$ purge, and without $N_2$ purge.

We noticed that the device was reviving only with the light after $NO_2$ exposure. It suggests that $NO_2$ is bonding with active IGZO film, and reviving only after application of external energy. The role of $N_2$ purge in revival is also crucial as we observed that the recovery is quicker in the presence of $N_2$. In the case of revival with the blue LED, devices were regenerating within 5 minutes. With the same intensity of light, the recovery is delayed for five more minutes in the absence of $N_2$ purge. It means that nitrogen was helping in sweeping away the neutralized $NO_2$ molecules after light-activated desorption.

**SI-5. Depth Profile of IGZO film was measured using high-resolution Rutherford backscattering spectroscopy and energy dispersive x-ray spectroscopy**

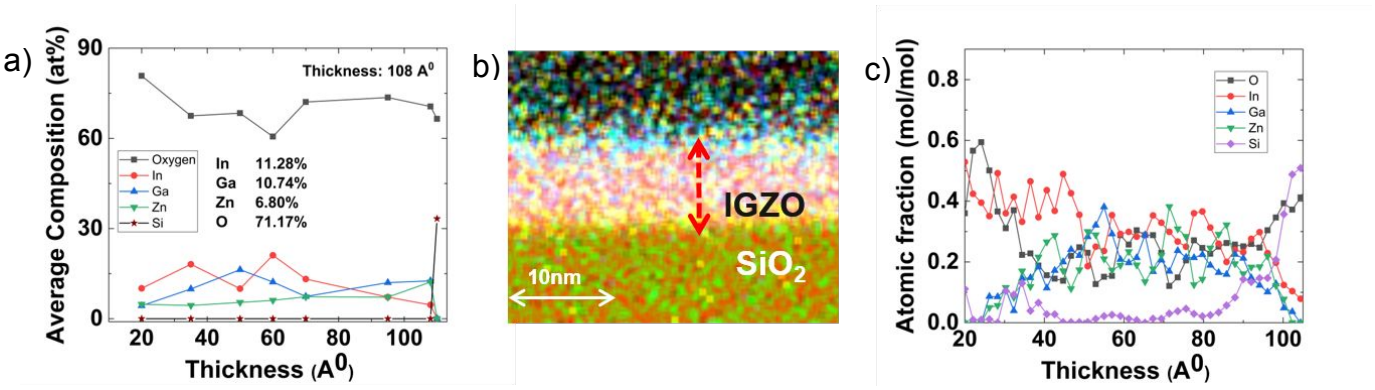


Figure S4. a) Depth Profile of IGZO measured using Rutherford backscattering spectroscopy b) Line profile overview image of the device stack cross-section showing the interface layers of IGZO and $SiO_2$ for of (EDX) spectroscopic analysis c) Line profile of IGZO layer indicating the highest Indium concentration at the surface

The average composition profile was measured using high-resolution Rutherford backscattering spectroscopy. It can be seen from the depth profile that after 10.8 nm, the abrupt change in the concentration of the In, Ga, Zn, and Oxygen for the accurate fitting of the spectra, which was the physical thickness of the IGZO thin film in the device stack. The indium concentration was vital for the adsorption of $NO_2$[2] at lower temperatures. This was also evident from the EDX analysis performed on the device stack shown in Figure S4c.

## SI-6. Effect of the x-ray on an unexposed and $NO_2$ exposed IGZO TFTs

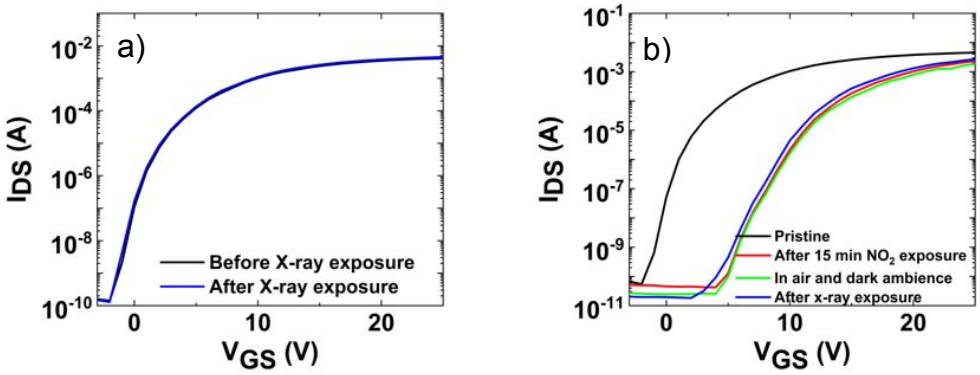


Figure S5. a) Transfer characteristics of the pristine device before and after exposure of x-ray for 4 minutes b) Transfer characteristics of IGZO TFT sensor after prolonged exposure to $NO_2$, showing the shift in threshold voltage in dark ambience after exposure and non-revival characteristics even after x-ray exposure.

## SI-7. Kelvin probe force microscopy analysis

The contact potential difference (CPD) is measured on the standard HOPG sample and extracted the work function of the tip.[3] Measured CPD can be defined as the following:

$$\text{CPD} = \frac{\emptyset_{tip} - \emptyset_{sample}}{e} \quad \text{(SE 6)}$$

Work-function of the tip is measured to be $\phi_{tip}$= 4.3153 eV

Work-function of the sample ($\phi_{sample}$) is measured from the CPD equation (Equation S6). Mean CPD values of the sample before and after $NO_2$ exposure of the samples are 0.2693 V and 0.3153, respectively.

A shift in the work function toward the vacuum level (E= 0 eV) indicates the presence of a negative charge on the surface due to ionized $NO_2$ molecules ($NO_2^-$). From the KPFM analysis, we conclude that $NO_2$ was absorbed on the surface of IGZO, as depicted in the schematic of the sensing mechanism (Figure 6a).

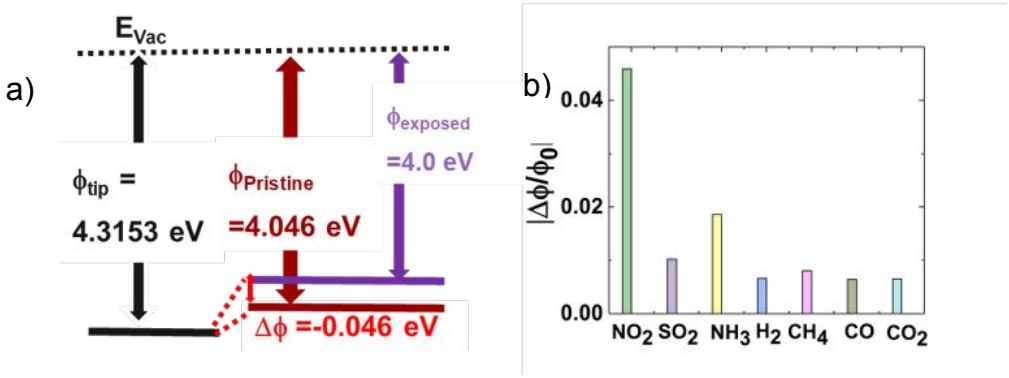


Fig. S6 a) Energy level schematic showing the difference in the work-function observed using KPFM (Pristine and NO2 exposed IGZO devices), b) The change in the work-function of IGZO thin film after exposing to various gases, showing dominant adsorption of the $NO_2$.

### SI-8. Fabrication process flow of microsystem

The silicon on insulator (SOI) substrate is the best choice in order to keep the material system same as discussed for IGZO TFT sensor. Even most of the fabrication processes except the process flow are same as IGZO TFT fabrication (SI-1). In the process flow of microsystem fabrication, top silicon device layer of SOI substrate serves as bottom gate electrodes and the buried oxide as isolation.

The process flow begins with the cleaning of SOI substrate to remove the organic and metal impurities by dipping them in the Piranha solution for five minutes and removal of native oxide using buffered oxide etch solution. The individual gate electrodes were patterned on SOI substrate with the doped device layer, and the etching of the silicon on the SOI substrate was performed using deep reactive ion etching (bosch process).

Later the process of thermal oxidation was performed in the thermal furnace that served as Gate oxide (~150 nm). The optimized IGZO deposition followed by annealing was performed as explained in the (SI-1). The openings were made to isolate the channel using contact aligner and IGZO was patterned using buffered $HF^4$ in such a way it also opens contact for gate electrode. Subsequently interconnects, contacts for source, gate, drain were patterned and deposited through liftoff process as explained in the (SI-1) with dimensions W = 583640 μm and L=10 μm.

The parlyene-c as a passivation layer is the best choice to employ IGZO TFT as a circuit element, without disturbing the IGZO properties by sputtering and to avoid the device subjecting to high temperature process. Hence one of the TFT passivated through chemical vapor deposition using shadow mask.

## References:


(1) Petti, L.; Münzenrieder, N.; Vogt, C.; Faber, H.; Büthe, L.; Cantarella, G.; Bottacchi, F.; Anthopoulos, T. D.; Tröster, G. Metal oxide semiconductor thin-film transistors for flexible electronics. *Applied Physics Reviews* **2016,** *3* (2), DOI: 10.1063/1.4953034.

(2) Li, Z.; Li, H.; Wu, Z.; Wang, M.; Luo, J.; Torun, H.; Hu, P.; Yang, C.; Grundmann, M.; Liu, X.; Fu, Y. Advances in designs and mechanisms of semiconducting metal oxide nanostructures for high-precision gas sensors operated at room temperature. *Materials Horizons* **2019,** *6* (3), 470-506, DOI: 10.1039/c8mh01365a.

(3) Surya, S. G.; Samji, S. K.; Dhamini, P.; Ganne, B. P.; Sonar, P.; Rao, V. R. A Spectroscopy and Microscopy Study of Parylene-C OFETs for Explosive Sensing. *IEEE Sensors Journal* **2018,** *18* (4), 1364-1372, DOI: 10.1109/jsen.2017.2786739.

(4) Lu, C.; Hou, T.; Pan, T. High-Performance Double-Gate $\alpha $ -InGaZnO ISFET pH Sensor Using a HfO2 Gate Dielectric. *IEEE Transactions on Electron Devices* **2018,** *65* (1), 237-242, DOI: 10.1109/TED.2017.2776144.